MEDICAL ROBOTS

Preventing pressure ulcers by increasing pressure: An unorthodox alternating-pressure mattress

Zhidi Yang[1]†, James L. Weida[1,2], Siyuan Shao[1], Brandon Reedel[1], Collin Shannon[1], Junlin Chen[1], Piyush Sheth[2], Jonathan B. Hopkins[1]*†

Despite the devastating effects of pressure ulcers (PUs), little is understood about how they can be prevented using alternating-pressure (AP) mattresses. Such mattresses typically aim to minimize the pressures imparted while alternating between different states of pressure to prevent areas of tissue from being persistently occluded of blood flow. In this work, we built an actuator bed to study AP approaches and learned that AP mattresses should aim to increase—not decrease—peak pressures to a certain extent if such areas are to be minimized for effectively preventing PUs. In addition, we learned that such mattresses should aim to increase the difference between their loading and off-loading pressures. We identified optimal parameters from the study and used them to design an AP mattress made of compliant mechanisms that markedly reduce areas of persistent occlusion by exhibiting relatively high peak pressures that are periodically alternated with substantially lower off-loading pressures. The mattress's performance was characterized and compared against a standard foam pad in its flat and raised configurations. The load required to actuate the mattress from one of its stable states of pressure to the other was also measured.

INTRODUCTION

Pressure ulcers (PUs), also known as bedsores, pressure injuries, or decubitus ulcers, are localized injuries to the skin or underlying tissue caused by unrelieved pressure leading to ischemia and tissue necrosis (*1*). In US acute care facilities alone, 2.5 million PUs are treated each year at a cost of $11 billion annually, surpassed only by the costs of cancer and cardiovascular diseases (*2*). PUs mostly occur in individuals with limited mobility (*3*) (the elderly, handicapped, injured, sick, obese, or those recovering from surgery) and are often accompanied by deleterious physical, psychological, and social consequences (*4*).

Despite the sizeable morbidity and mortality that PUs inflict (60,000 deaths per year) (*5*), they are preventable. Although numerous factors collectively affect the formation of PUs, as detailed in the Supplementary Materials, the most prevalent factor that can be addressed by support-surface technologies is perfusion (*6*). If the surface supporting the patient does not impart pressures that exceed the threshold at which blood and other lymphatic fluids are occluded to the patient's tissue (*7*), or if it does impart such pressures but not persistently over a prolonged period of time (*8*, *9*), perfusion is maintained and the risk of developing PUs is reduced. This occlusion pressure threshold (OPT), which corresponds to capillary filling pressure, varies in individuals from 20 to 40 mmHg (*10*), with an average value of 32 mmHg (*10*–*13*). Thus, it is recommended that patients be repositioned every 2 hours for providing pressure relief to areas that could exceed 32 mmHg (*7*, *13*). Adherence to this policy, however, is cumbersome and costly and thus typically occurs only 66% of the time (*7*). Moreover, turning the patient can injure the caregiver (*7*, *14*) and harm the patient's skin because of dangerous shearing loads, which should also be avoided for preventing superficial PUs (*7*, *13*, *15*).

Numerous PU prevention devices have been proposed to address these issues (*7*, *16*). Some devices aim to periodically reposition the patient by inclining or turning them (*17*–*19*). Other devices attempt to relieve pressure directly without moving or disturbing the patient from their sleep. These pressure-relieving devices are categorized as passive or active (*7*). The passive devices, also known as reactive, constant low-pressure, or static pressure-reducing devices, naturally conform to patients via gravity and thereby reduce pressure as the contact area increases with immersion. Examples include support surfaces that are filled with various combinations of foam, gel, fiber, air, water, or beads (*20*, *21*). The active devices undergo dynamic changes either manually or via automated actuation to relieve pressure directly. Alwasel *et al.* (*22*) proposed a mattress with a section of cubes that can be manually extracted from under the patient to control pressure distribution. Moon *et al.* (*23*) proposed a mattress consisting of tubes arranged in sections that are inflated via pressures calculated from the patient's height and weight using anthropometric data. Some of the most advanced active devices use pneumatic (*24*–*35*) or electromechanical (*36*–*41*) actuators in conjunction with embedded pressure or force sensors to continually readjust and minimize the peak pressure imparted on the patient in real time via closed-loop control.

Devices that solely attempt to minimize peak pressure, however, often fail to prevent PUs if the patient's OPT is less than the peak pressure achieved because such devices persistently occlude blood flow where the peak pressure is applied (*6*). Active pressure-relieving devices that periodically alternate between different states of pressure are often favorable because they reduce the chance that any one location on the patient's body will be subjected to a persistent pressure above the patient's OPT for a prolonged period of time (*42*, *43*). Furthermore, such alternating-pressure (AP) devices do not require sensors or closed-loop-control circuitry because they simply alternate between their different states of pressure and are thus more practical, cost-effective, and robust than the more advanced active devices mentioned previously. Consequently, some of the most popular mattresses used for preventing PUs [aside from air-fluidized beds, which are often prescribed to treat the most severe PUs but

[1]Mechanical and Aerospace Engineering, University of California, Los Angeles, Los Angeles, CA 90095, USA. [2]K Medical LLC, Porter Ranch, CA 91326, USA.
†These authors contributed equally to this work.
*Corresponding author. Email: hopkins@seas.ucla.edu

weigh more than half a ton (450 kg), cost >$50,000, and are not suited for home care use] are AP mattresses. These mattresses typically consist of transversely aligned tubes that periodically inflate/deflate to alternate areas of high pressure. Overlays with similarly alternating bladders are also commonly used (*44*).

Despite their popularity, however, limited studies exist to understand what factors affect the performance of AP devices and how such devices can be improved to definitively prevent PUs. As a result, existing AP products fall short of their potential and fail to produce consistent evidence of convincing efficacy (*9*, *45*). Fundamental studies, however, indicate that the concept of alternating pressure is uniquely promising for preventing PUs by facilitating and even enhancing perfusion. Jan *et al.* (*8*) demonstrated that alternating pressure between 0 and 60 mmHg achieved improved perfusion compared with holding a constant pressure of 30 mmHg. Pauly *et al.* (*9*) demonstrated that alternating pressure between 5 and 75 mmHg on sacral skin achieved improved perfusion compared with alternating pressure between 15 and 65 mmHg. Mayrovitz and Sims (*42*) demonstrated that cyclically pressurizing heels produced greater blood perfusion compared with a resting baseline. Bader (*43*) demonstrated that cyclic loading of the sacrum produced rapid and complete tissue recovery in both healthy and debilitated participants—although some debilitated participants did experience impaired tissue recovery. Chai *et al.* (*46*) inflated two different configurations of four bladders using three different pressure combinations over three different cycle periods to better understand factors that govern the performance of inflatable AP devices specifically. Other studies have focused on characterizing the performance of specific AP designs (*47*, *48*).

In this work, a bed consisting of 1260 independently controlled linear actuators was created (Fig. 1A) to rigorously study the geometric factors (specifically, the spacing between alternating peaks) that affect the PU prevention capabilities of AP technologies and thereby to learn how to improve their ability to facilitate perfusion. The bed's actuators were programmed to impose two states of undulating checkerboard-like surface patterns on an anatomically correct dummy in supine position (fig. S1), where the peaks of one state alternate with the pits of the other state (Fig. 1A). The pitch, *P*, and depth, *D* (fig. S2), of these surface patterns (that is, the horizontal spacing between their neighboring peaks and the vertical spacing between their pits and peaks, respectively) were swept to determine which combination of these parameters would best facilitate perfusion (movie S1). It was postulated that perfusion is best facilitated using surface-pattern parameter combinations that minimize the overlapping areas where pressures commonly reach or exceed the OPT in both states of alternating pressure. Such areas occur where no pressure relief is experienced below the OPT no matter how often the different states of pressure are alternated and thus are the areas where blood flow is persistently occluded. As such, the sum of these areas is called the area of persistent occlusion (APO) and is a measure of the region size in which PUs are most likely to form. From this study, it was determined that AP devices that impart higher peak pressures tend to reduce both the APO and the APO sensitivity to OPT values that vary between 20 and 40 mmHg and thus tend to be more effective at preventing PUs than AP devices that aim to minimize peak pressures. Moreover, it was determined that AP devices that achieve larger differences in loading and off-loading pressures when alternated between different states also tend to be more effective at reducing APO. These findings, along with the optimal *P* and *D* values identified from the study, informed the design of a practical, low-cost mattress (Fig. 1B and fig. S3) that achieves two alternating checkerboard-like surface patterns, which each impart unconventionally high—but comfortable—peak pressures that alternate to markedly lower off-loading pressures as a result. The mattress consists of compliant mechanisms (*49*, *50*) that enable it to be smoothly transitioned from one state of pressure to the next with minimal energy (movie S2), thus enabling easy manual or automated actuation by caregivers or low-powered motors, respectively. Experiments were conducted to compare the mattress's peak pressure, APO, and APO sensitivity against a standard foam pad in

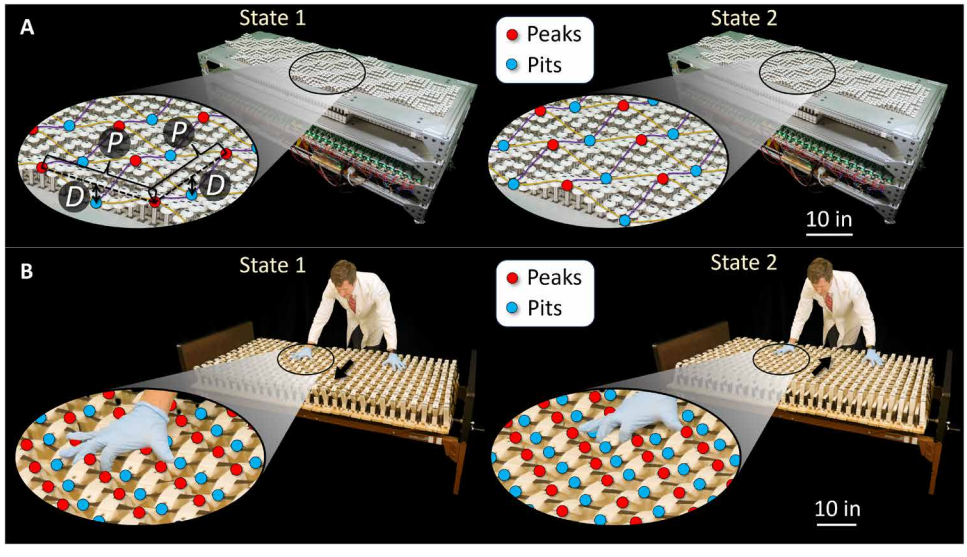

Fig. 1. Actuator bed and the compliant-mechanism mattress that it helped design. (**A**) A bed consisting of 1260 linear actuators, which can collectively achieve programmable surface patterns, was built to study the PU prevention approach of alternating pressure between two undulating checkerboard-like states of pressure and to identify optimal *P* and *D* values. (**B**) An AP mattress consisting of compliant mechanisms was designed using the optimal values identified for most effectively preventing PUs. Scale bars, 10 inches (25.4 cm) [(A) and (B)].

both flat and head-and-knee-raised configurations. Because APO and APO sensitivity were used as metrics to gauge PU prevention efficacy in this work, and because these metrics depend on the size, shape, stiffness, and weight of the body lying on top of an AP device—not the response of living tissue—an anatomically correct dummy was used instead of living participants to remain still as data were collected over many days. A more detailed discussion about the decision to use a dummy instead of living participants for the studies of this work is provided in the Supplementary Materials.

RESULTS

Compliant-mechanism mattress

Although others have proposed pressure-relieving mattresses made of rigid mechanisms (*36*, *51*), which consist of bodies joined together by sliding and/or rolling contact joints, the AP mattress of this work (Fig. 2A) is made of compliant mechanisms (*49*, *50*), which consist of bodies joined together by flexible joints that deform to achieve desired motions, for the reasons discussed in the Supplementary Materials. The mattress consists of two unique panel designs (Fig. 2B), which are alternated and spaced a distance that is half of the mattress's intended pitch, $P/2$, along its length (Fig. 2A). Both designs consist of the same repeating trapezoidal pattern of connected bodies, but the configuration of one panel is offset from the pattern of the other by the same distance, $P/2$ (Fig. 2B), so the mattress can achieve the checkerboard-like surface pattern desired. Specifically, each panel consists of angled rigid struts that join with a fixed base on one end and top bars on the other end (Fig. 2C) via flexure hinges (Fig. 2A) that locally deform to achieve rotations. The flexure hinges (*50*) of this work's prototype are made from metal shims (fig. S4 and movie S3) as detailed in Materials and Methods. Although neighboring struts should not be parallel for the mattress to properly function, every other strut should be parallel when the top bars are aligned as shown in Fig. 2C. If the mattress is compressed under a patient's weight (Fig. 2D), all of the panels will shift either to the right (fig. S5A) or to the left (fig. S5B) until hard stops (Fig. 2C) are engaged and the mattress settles into one of its two stable states with the desired undulating surface pattern manifested. The peaks of each pattern will alternate to the pits of the other pattern and vice versa as the mattress is actuated between states. No shearing forces are imparted on the patient's skin in the process because their body moves with the top surface of the mattress. A foam pad should also be used on the mattress to increase comfort and shield the patient from other unwanted loads. Although the top bars (fig. S6) are intended to rigidly resist compression, the current prototype allows them to extend a distance along their axes when they are loaded in tension (movie S4) to allow the mattress's pitch and depth to remain uniform (fig. S7) underneath the patient as detailed in the Supplementary Materials. It is expected that each panel within the final product will be injection molded as one part, like the 3D-printed preliminary concept shown in fig. S8, which is also discussed in the Supplementary Materials, to simplify the manufacturing process and fully leverage the advantages of compliant mechanisms (movie S5). The panels are inserted between a series of side flexures (fig. S9) on either side of the mattress along its length using press-fit features. These side flexures, detailed in Materials and Methods, are designed to guide the relative rotations (Fig. 2E) between neighboring panels about axes that lie on the top surface of the mattress (movie S6) to allow the mattress's head and knee portions to be raised (fig. S10) without pinching the patient or altering the desired surface pattern (movie S7). The kinematics enforced by these side flexures also accommodate stretch-resistant straps (Fig. 2E), which are threaded through slits in each top bar (fig. S6) for stabilizing their panels and ensuring that they all displace the same direction when the mattress is actuated.

Principles of static balancing (*52*, *53*) are leveraged to counteract the patient's weight using snap-on springs (Fig. 3A) that attach to the mattress's panels (Fig. 3B) via magnets embedded in square

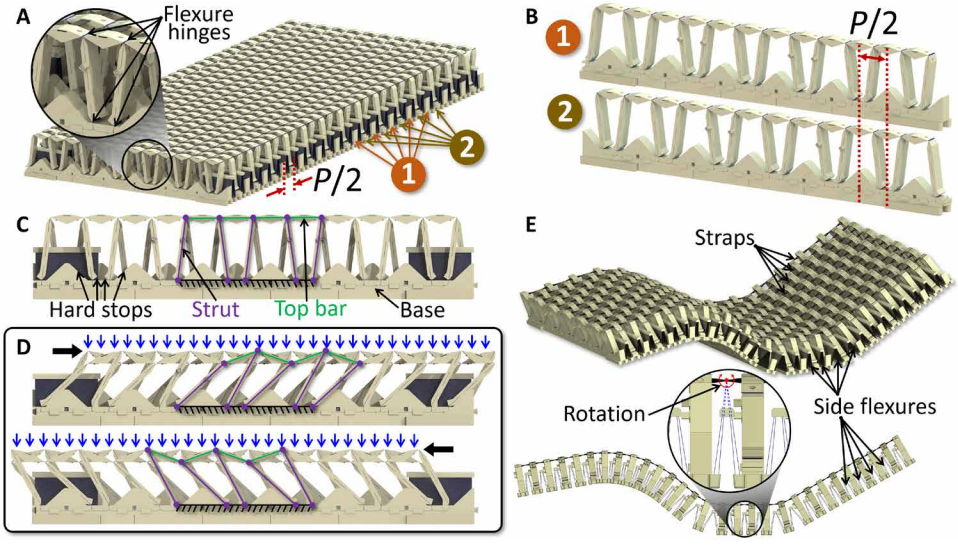

Fig. 2. How the compliant-mechanism mattress works. (**A**) The mattress consists of (**B**) two panel designs that (**C**) are made of bodies arranged in repeating trapezoid configurations, which when actuated (**D**) to the right or left produce an alternating checkerboard-like surface pattern of peaks and pits. (**E**) The panels are inserted between side flexures that deform to enable the head and/or knee portion of the mattress to be raised and lowered while still achieving the desired alternating pattern on its top surface.

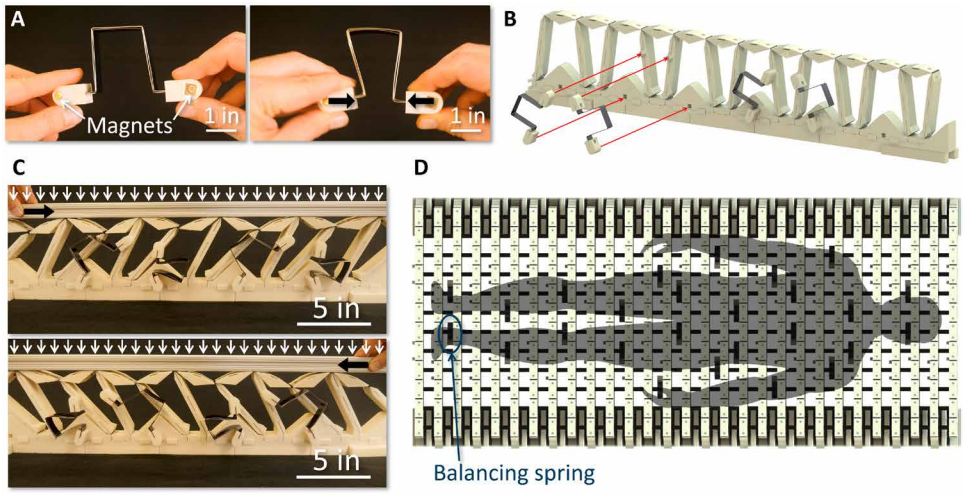

Fig. 3. Balancing springs markedly reduce the mattress's actuation energy. (**A**) Each spring consists of bent steel sheets attached to magnetic ends that (**B**) easily snap onto panels at different locations so that the mattress can be smoothly actuated (**C**) from one undulating state to the next with minimal actuation loads, because the weight of the patient and mattress is counterbalanced by the force of the deformed springs. (**D**) A software tool determines the optimal number and location of these springs within the mattress given the patient's height and weight. Scale bars, 1 inch (2.54 cm) (A) and 5 inches (12.7 cm) (C).

posts (fig. S4A) and mating holes (movie S8). If the optimal number of such balancing springs is properly used, they can markedly reduce the force required to actuate the mattress with a patient lying on top from either of the mattress's stable states on the right or left side (Fig. 3C) to its undeformed but higher gravitational-potential-energy state in the center (Fig. 2C). Moreover, the springs enable the patient to be gently lowered from this central state into the mattress's alternate stable state on the other side, where the panel hard stops should only gently engage under ideally balanced circumstances to avoid impact jolts. A software tool (fig. S11) was developed (software S1 available on Zenodo) using anthropometric data (*54*), as discussed in the Supplementary Materials, to determine the optimal number of balancing springs to use and where to place them (Fig. 3D) to minimize the force required to actuate the mattress with a patient on top. In addition to reducing the force of manual actuation, balancing springs also enable the automated actuation of the mattress (movie S9) via a few low-powered linear actuators, which are detailed in Materials and Methods and attach to the panels at similar locations as the springs (fig. S12). A discussion comparing the advantages of the mattress of this work with other AP technologies is provided in the Supplementary Materials.

Actuator bed study

An actuator bed (fig. S13) was designed and built (Fig. 1A) to study factors that affect the PU prevention capabilities of AP technologies and to identify what parameters (such as the P and D values) to apply to the mattress design of this work to best prevent PUs. Detailed descriptions of the bed's constituent parts (fig. S14) and control electronics (fig. S15) are provided in Materials and Methods. A software tool (fig. S16), developed to conduct the study (movie S10), is also provided (software S2 available on Zenodo) and discussed in the Supplementary Materials. A foam pad was placed on top of the actuator bed, followed by a pressure-sensing mat and a dummy (fig. S17 and Fig. 4A) as detailed in Materials and Methods. The bed's actuators were then controlled, as described in the Supplementary Materials, to collectively exhibit undulating checkerboard-like surface patterns, which would alternate between two different states, where peaks would become pits and vice versa (Fig. 1A), for specific P and D values. These values were swept (movie S1) from $P = 2$ to 24 inches (5.08 to 60.96 cm) and $D = 0.25$ to 1.5 inches (0.635 to 3.81 cm), respectively, and their corresponding surface patterns were offset to four different locations underneath the dummy for each scenario as discussed in the Supplementary Materials. The pressure-sensing mat collected data (movie S11) from each surface pattern's two states of alternating pressure (for example, Fig. 4B), and their corresponding APO was calculated for an OPT of 32 mmHg. In other words, the number of overlapping sensor-mat pixels that commonly reached or exceeded 32 mmHg in both states of alternating pressure was identified and then multiplied by 0.25 inches^2 (0.635 cm^2)/pixel because each pixel in the mat is 0.5 inches by 0.5 inches (1.27 cm by 1.27 cm). The highest pressure sensed in either state of each surface pattern (that is, the peak pressure) was measured and plotted (Fig. 4C) against these APO values. The trend of the resulting plot demonstrates that checkerboard-like AP mattresses that exhibit higher peak pressures tend to reduce APO. This general trend remains regardless of how the OPT varies in individuals between 20 and 40 mmHg (fig. S18).

If the same peak pressures are plotted against their corresponding APO sensitivity to OPT at an OPT of 32 mmHg (Fig. 4D), a similar trend is observed (that is, higher peak pressures tend to reduce APO sensitivity as well). This sensitivity can be identified by plotting the APO measured from each surface pattern against OPT values between 20 and 40 mmHg (fig. S19) and then by calculating the absolute value of the derivative (that is, the slope) of those plots at 32 mmHg. The trend remains when peak pressures are plotted against the absolute values of the best-fit line slopes of the corresponding data plotted in fig. S19 as an alternative measure of APO sensitivity to OPT between 20 and 40 mmHg (fig. S20).

When the absolute values of the pressure differences at every pixel on the pressure-sensing mat measured in both alternating states were averaged and plotted against the APO at an OPT of 32 mmHg

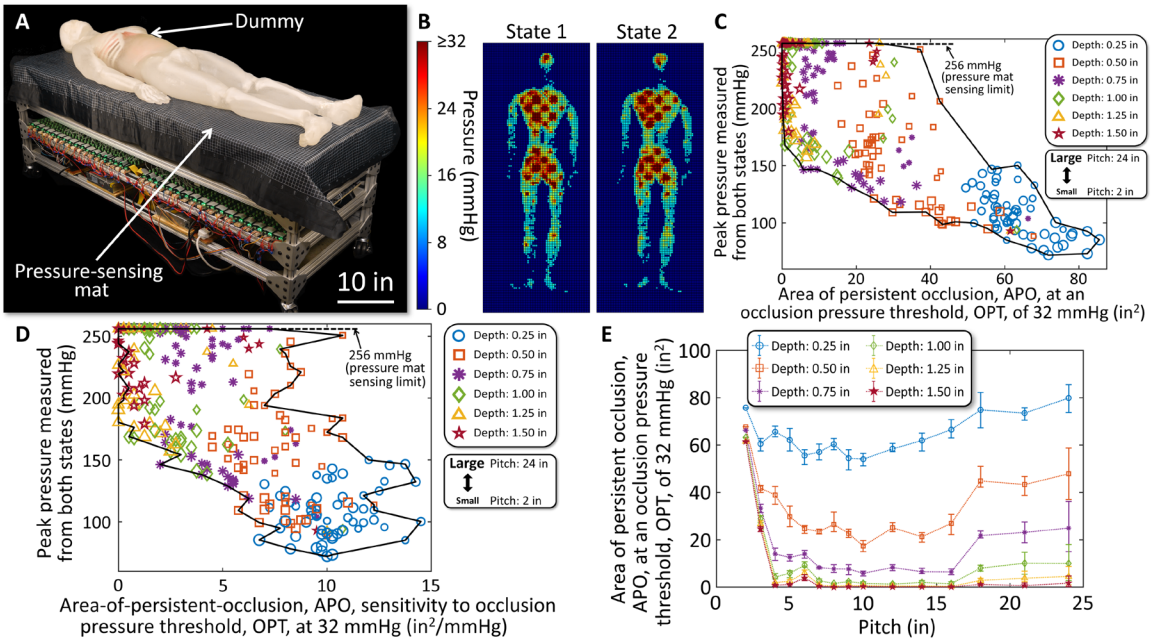

Fig. 4. Actuator bed study results. (**A**) A dummy, pressure-sensing mat, and foam pad were placed on a bed of actuators, which swept through numerous undulating checkerboard-like surface patterns that alternated between two states. (**B**) Pressure data measured from the two states of one such surface pattern example with a 5-inch (12.7-cm) pitch; a 1.5-inch (3.81-cm) depth; and a 2-inch (5.08-cm) and 0-inch row and column offset, respectively. The peak pressures of all of the data collected were plotted against (**C**) APO and (**D**) APO sensitivity to OPT at an OPT of 32 mmHg. The trend of both plots shows that APO and APO sensitivity are reduced by AP mattresses that exhibit higher peak pressures. (**E**) The APO-versus-pitch plot for different depth values shows which parameter combinations are best applied to AP mattresses that aim to reduce APO at an OPT of 32 mmHg. The trend lines in (E) pass through average values, and the error bars represent maximum and minimum values from a sample size of four, corresponding to each offset. Scale bar, 10 inches (25.4 cm) (A).

for each scenario swept (fig. S21), a similar trend was observed. The plot shows that checkerboard-like AP mattresses that achieved larger differences in loading and off-loading pressures tended to reduce APO. The data of fig. S21 were even more tightly circumscribed by their boundary along the trend direction than the data of Fig. 4 (C and D), which suggests an even stronger correlation.

The APO for all surface patterns swept at an OPT of 32 mmHg was also plotted against pitch for different depths (Fig. 4E) to aid in the identification of the best parameter combination to apply within the AP mattress design of this work. The same parameter-sweep study was conducted using the dummy but without foam (movie S12) to determine the effect of foam on the results (figs. S22 and S23) as discussed in the Supplementary Materials. Different ranges of depth and offset values (fig. S24) were also swept without foam (movie S13) to determine the effects of offsetting the surface pattern relative to the dummy (fig. S25), as is also discussed in the Supplementary Materials.

Mattress design and performance comparison

A software tool (fig. S26) was created (software S3 available on Zenodo) to generate trapezoidal panel designs (for example, Fig. 2C) that achieve desired *P* and *D* values (movie S14) as discussed in the Supplementary Materials. A *P* of 5 inches (12.7 cm) and a *D* of 1 inch (2.54 cm) were used with this software to design the compliant-mechanism mattress of Fig. 1B for the reasons also discussed in the Supplementary Materials. Details regarding the design's constituent parts (fig. S27) are provided in Materials and Methods along with a description of the setup used to characterize the mattress's performance (Fig. 5A). This setup (fig. S28) consisted of a bed frame; a series of planks joined together by straps (fig. S29), which form rolling-contact joints (*55*); the mattress itself; a foam pad; a pressure-sensing mat; and a dummy. The dummy was randomly placed in 10 different locations on this compliant-mechanism–mattress setup, and the pressure-sensing mat collected data (movie S15) for each location (for example, Fig. 5A) in both states of alternating pressure (Fig. 1B). The results were compared against a different setup (Fig. 5B) consisting of a bed frame, wooden boards, a foam pad, a pressure-sensing mat, and a dummy (fig. S30) as detailed in Materials and Methods. Again, the dummy was randomly placed in 10 different locations on this foam-pad setup (for example, Fig. 5B), and the pressure-sensing mat collected data (movie S16) for each location. The peak pressures (Fig. 5C) measured from both states of the compliant-mechanism mattress (fig. S31A) were found to be higher (~161 mmHg) and exhibited more variability than the foam pad's peak pressures (~40 mmHg) (fig. S31B). The APO values for both the mattress (fig. S32A) and foam pad (fig. S32B) were averaged and plotted for OPT values between 20 and 40 mmHg (Fig. 5D). The APO and APO sensitivity of the mattress at 32 mmHg were 0.725 inches^2 (1.84 cm^2) and 0.2 inches^2 (0.51 cm^2) per mmHg, respectively. In contrast, the foam pad's APO and APO sensitivity at 32 mmHg were substantially higher at 24.65 inches^2 (62.6 cm^2) and 6.7 inches^2 (17.02 cm^2) per mmHg, respectively. Thus, patients with an OPT > 28 mmHg would not likely acquire PUs if they used the mattress but would likely acquire PUs if they used the foam pad unless their OPT was > 38 mmHg. The APO at an OPT of 32 mmHg was also measured from the two

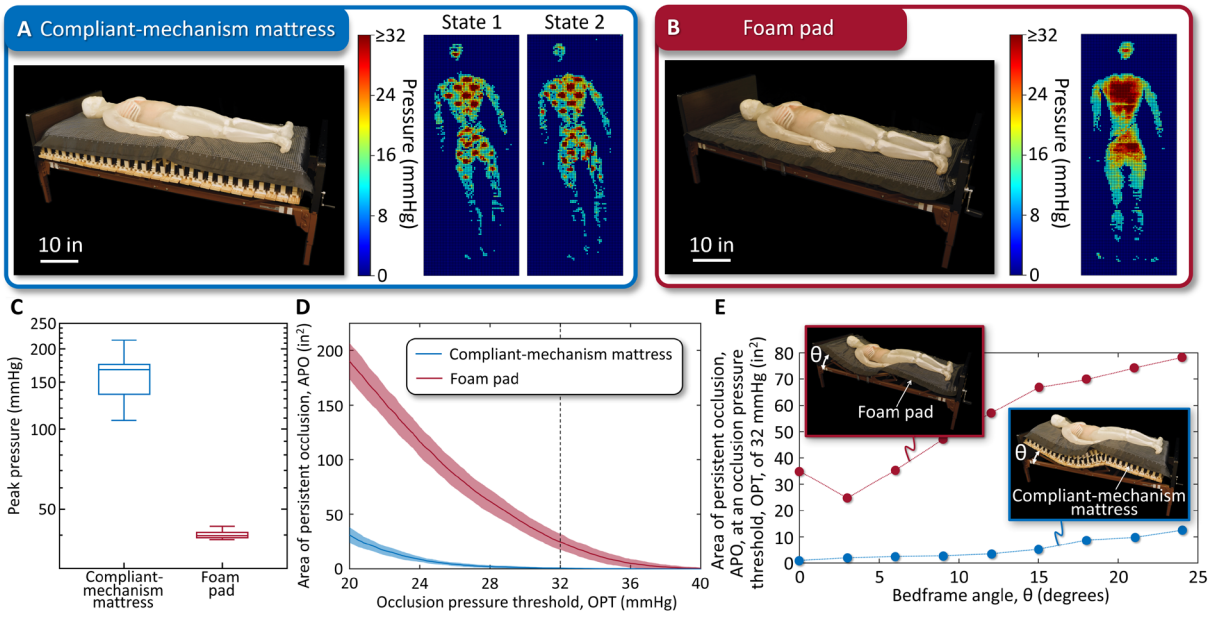

Fig. 5. Comparison between the compliant-mechanism mattress and the foam pad. Pressure data taken (**A**) from the compliant-mechanism mattress's two alternating states and (**B**) from the foam pad for when the dummy was placed in one of the 10 different locations on each support surface. A comparison of (**C**) the peak pressures and (**D**) the APO plotted against the OPT as measured from the compliant-mechanism mattress and the foam pad during each of their 10 dummy-relocation trials. Thus, the box plot of (C) was generated using a sample size of 10. The central marks represent the median values, the bottom and top edges of the boxes represent the 25th and 75th percentiles, respectively, and the lower and upper whiskers represent the minimum and maximum values, respectively. The solid lines in (D) represent the mean APO, and the shaded areas represent 1 SD calculated from the sample size of 10. (**E**) A comparison of the APO at an OPT of 32 mmHg measured from the mattress in its two stable states and from the foam pad as the bed frame was raised over a range of angles. As the head portion of the bed frame is raised an amount, θ, the knee portion is coupled to raise with a 3:2 head-to-knee angle ratio. Scale bars, 10 inches (25.4 cm) [(A) and (B)].

states of the mattress and from the foam pad as the dummy was raised by the bed frame (movie S17) over an angle, θ (Fig. 5E). Although the mattress's APO does increase as the angle increases, it increases at a lower rate than the foam pad, and thus, the mattress would be substantially more effective at preventing PUs even when the bed frame is elevated. A system of cords and pulleys was constructed (movie S18) to measure the force required to successfully actuate the mattress from one state to the next with the 220-lb (99.79-kg) dummy lying on top (Fig. 6A) using the configuration of balancing springs shown in Fig. 3D as detailed in Materials and Methods. A force of 19 lbf (84.5 N) was found to work >90% of the time (Fig. 6, B to D).

DISCUSSION

The actuator bed study of this work demonstrated that AP devices with checkerboard-like surface patterns that impart higher peak pressures are generally more likely to prevent PUs than those that aim to minimize peak pressures. This finding results from the fact that surface patterns that achieve higher peak pressures tend to also produce lower APO (Fig. 4C) and APO sensitivity (Fig. 4D) values when the pattern is alternated. The study also found that AP devices that achieve larger differences in loading and off-loading pressures when alternated between their different states of pressure also tend to be more effective at preventing PUs in that they also tend to reduce APO (fig. S21).

It may seem to be an unfortunate finding that, to reduce a patient's APO and APO sensitivity, it is simultaneously necessary to provide the patient with an AP mattress that imparts higher peak pressures, because intuitively one would think that higher pressures are harmful in preventing PUs. However, recent studies conducted on living participants found that higher peak pressures that are alternated with lower off-loading pressures imparted at a single point on the sacrum can produce improved blood perfusion in the skin (*9*), even when compared with lower pressures that are held constant (*8*). Such peak pressures should, however, not approach pressures that could cause immediate bruising or damage to skin and must be alternated with sufficient frequency to allow the necessary occlusion relief. More studies are necessary to definitively identify what that frequency should be for a given patient, but regardless of its value, the cycle time does not affect the design of the AP-compliant mechanism mattress of Fig. 1B or the results of the actuator bed study for the reasons detailed in the Supplementary Materials. Thus, cycle time is not a focus of this work. Last, despite these findings, it remains advisable to minimize the peak pressures imparted by AP devices for the sake of comfort so long as those peak pressures are high enough to eliminate APO for OPT values between 20 and 40 mmHg.

The AP-compliant mechanism mattress, designed and fabricated using the results of the actuator bed study, achieved an APO that is 34 times smaller than the APO achieved by a standard foam pad at an average OPT of 32 mmHg. That APO remained low compared with the foam pad regardless of how the bed frame was elevated. Balancing springs reduced the load required to actuate the mattress to <9% of the user's weight. These results indicate the promise of the AP mattress introduced.

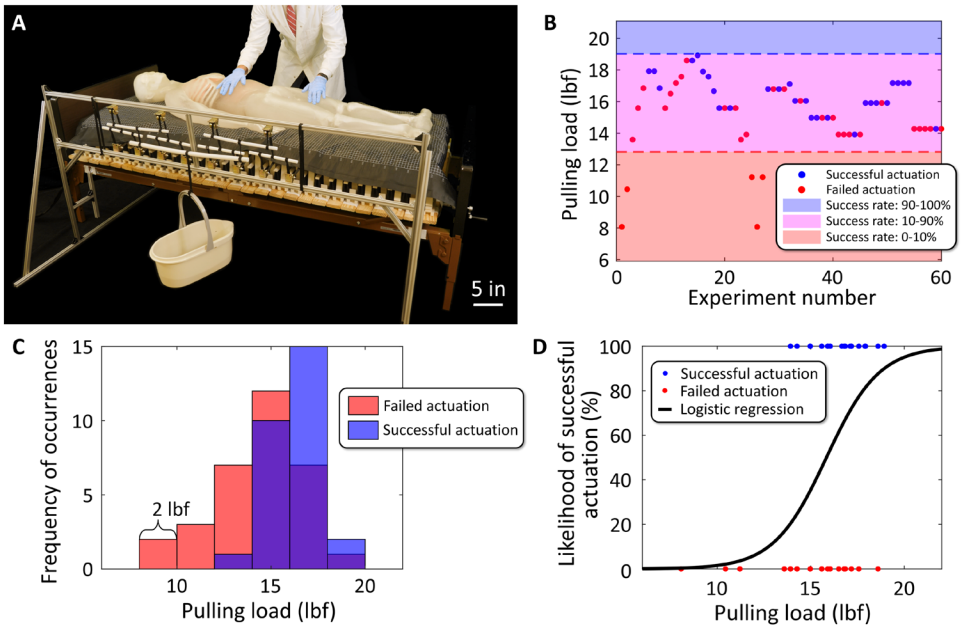

Fig. 6. Measuring the load required to actuate the mattress with balancing springs. (**A**) The experimental setup used to measure the load required to actuate the compliant-mechanism mattress consisted of a whippletree system of pulleys and cords that uniformly pull on the mattress's foam pad according to the weight placed in the bucket. (**B**) The pulling loads observed for 60 different experiments when the mattress was equipped with an optimal number and arrangement of balancing springs. The same successful and failed actuation data plotted as (**C**) a histogram and (**D**) a logistic regression curve. Scale bar, 5 inches (12.7 cm) (A).

MATERIALS AND METHODS

Mattress flexure hinges

This section describes how the mattress prototype of Fig. 1B was made to achieve robust flexure hinges (Fig. 2A) at the junctions of each of its panels' rigid bodies so that it could successfully deform over large ranges of motion while supporting the weight of patients when actuated from one stable state to the next (movie S3). Long metal shims were cut, bent, and punched before being inserted inside thin slots fabricated within the rigid parts that constitute each panel (fig. S4A). Plugs with matting slots were press-fit inside the struts and bases of the panels using Gorilla Clear Grip contact adhesive to keep the metal shims in place. Bolts and mating nuts were used with Gorilla 5-min epoxy to firmly attach the two ends of the metal shims inside the slots on either end of the top bars within each panel. All of the parts, colored with a yellow hue in fig. S4A, were additively fabricated from Vanilla White Prusament polylactic acid (PLA) filament using a Prusa i3 MK3S+ 3D printer. The metal shims were 1095 spring steel strips that were 1 inch (2.54 cm) wide and 0.002 inches (0.005 cm) thick (fig. S4B). They were permanently bent in place using a USATCO Bendito 1824 sheet metal brake, and their bolt holes were punched using a McMaster-Carr compact portable lever-operated hole punch 3461A22. In this way, the metal shims were able to produce robust, tear-resistant flexure hinges that successfully achieved relative rotational degrees of freedom (DOFs) between each panel's rigid bodies over sufficiently large ranges of deformation without yielding (fig. S4C).

Mattress side flexures

This section explains the design, fabrication, and function of the mattress's side flexures, labeled in Fig. 2E (movie S6). These side flexures consist of two repeating patterns of four metal blade flexure units that join each panel section together along the length of the mattress on both of its sides (fig. S9A). The panels were inserted between the side flexure units using double-diamond press-fit features, as shown by the red arrows in fig. S9A. In each of the side flexure's units (fig. S9B), one pair of 0.015-inch-thick (0.038-cm-thick) blade flexures (*50*), made of 1095 spring steel, join a panel section to an intermediate rigid body that was then serially joined to the neighboring panel section by another pair of blade flexures. These flexures were press-fit and glued using Gorilla clear grip contact adhesive inside slots within their rigid bodies, which were additively fabricated from Vanilla White Prusament PLA filament using a Prusa i3 MK3S+ 3D printer. Each pair of blade flexures permits a single rotational DOF only along a common axis that is located on the top surface of the mattress when it is actuated to one of its two stable states (Fig. 2E). The axis is centered between the unit's two panels and is parallel to the direction along their length. The blade flexures enforce this DOF because the planes on which they lie all intersect along the DOF's rotational axis as shown in Fig. 2E. Thus, because each pair of blade flexures achieves a redundant rotational DOF in their serially configured unit (fig. S9B), when the units are combined (fig. S9C), they can collectively deform substantial amounts about their axes in either direction without yielding. Thus, the side flexures permit the mattress to be lowered (fig. S10A) and raised (fig. S10B) in both the head and knee portions regardless of where the bed frame's joints may be located or how the mattress may be positioned on any bed frame design.

It is important that the axes of rotation enforced by the side flexures be positioned on the top surface of the mattress when it is actuated to either of its stable states as shown in Fig. 2E for three reasons. First, the farther the rotational axes are above or below the mattress surface, the more the top of the panels will displace toward or away

from each other as the mattress is raised or lowered and thus the more pinching and/or shearing the patient will experience. Thus, to reduce this pinching and shearing as much as possible, it is important that the axes lie on the top surface of the mattress when it is actuated to one of its two stable states (that is, the configuration of the mattress when a patient is lying on it as it is being raised or lowered). Second, it is important that the rotational axes are located in this way so that the desired pitch of the checkerboard-like undulating surface pattern changes as little as possible as the mattress is raised or lowered. Last, it is important that the rotational axes lie on the mattress's top surface so that the stretch-resistant straps, labeled in Fig. 2E, are not forced to attempt to stretch as the knee portion of the mattress is raised. The straps, which are threaded through slits in each of the panels' top bars (fig. S6A), should be as stretch resistant as possible so that all of the panels are coupled together and are thus forced to actuate in the same direction. After the head and knee portions of the mattress are raised, it is important that the mattress can still be actuated to either of its stable states and exhibit the desired alternating checkerboard-like surface pattern without jamming (movie S7).

Actuators used to automate the actuation of the compliant-mechanism mattress

This section describes how linear actuators are used to automate the process of switching the mattress between its two stable states (movie S9). An example linear actuator is shown attached to a portion of a mattress panel in fig. S12A. The actuator is a P16-P linear actuator with feedback from Actuonix Motion Devices. Its range is 150 mm, its maximum axial load capacity is 300 N, its maximum speed is 4.8 mm/s, and its gear ratio is 256:1. It attaches to the panel's base at one end and to one of the panel's struts on the other end. As it extends or contracts, it drives the panel to the right (fig. S12B) or to the left (fig. S12C) side, respectively. So long as the mattress is equipped with the optimal number and arrangement of balancing springs according to the patient's weight and height, only a few of these low-powered actuators spaced regularly throughout the mattress's panels are necessary to actuate the mattress with the patient lying on top. The actuator in fig. S12A joins to the panel using special attachments (fig. S12D), which were additively fabricated from ESUN Red PLA+ filament using a Prusa i3 MK3S+ 3D printer. The attachments consist of two pairs of opposing parts that are bolted together onto the panel's base or strut. They use flexures (*50*) that accommodate assembly imperfections and help prevent the actuators from experiencing harmful off-axis loads. They also allow more compliance in the panels that are connected to the actuators whether they are extending, contracting, or are locked in place.

Actuator bed's constituent parts and control electronics

This section describes the parts and control electronics that constitute the actuator bed (Fig. 1A) used to study the approach of alternating pressure to prevent PUs. A computer-aided design (CAD) model of the assembled actuator bed with its various constituent parts is shown in fig. S13, and an exploded view of the parts is shown in fig. S14. The actuator bed's supporting structure is mounted on caster wheels and consists of T-slot aluminum framings with rail dimensions of 1.5 inches by 1.5 inches (3.81 cm by 3.81 cm). Two 0.25-inch-thick (0.635-cm-thick) aluminum plates are secured to the framings using aluminum brackets. A waterjet was used to cut holes in the two aluminum plates to align and fix 1260 12-V electric linear microactuators (Progressive Automations, PA-07-4-5) between them. The shaft of these actuators can extend and contract over a range of 4 inches (10.16 cm), can travel with a maximum speed of 0.6 inches/s (1.52 cm/s), and can exert a dynamic load of 5 lbf (22.24 N). The actuators are arranged side by side with a center-to-center spacing of 1 inch (2.54 cm) between neighboring actuators along both the row and column directions, which correspond to the x and y axes labeled in the coordinate system of fig. S13, respectively. The shaft of each actuator is fitted with a cap, which was additively fabricated from Vanilla White Prusament PLA filament using a Prusa i3 MK3S+ 3D printer. These caps were designed to more evenly spread out the pressures between the ends of the actuator shafts to more closely mimic a continuous surface because it was not possible to move the actuators any closer together. Each actuator is connected to a pluggable terminal block on custom-designed actuator-controller (fig. S14) printed circuit boards (PCBs) (fig. S15A), which are equipped with motor drive integrated circuits (ICs) and protective circuits. Each PCB is, in turn, connected to several 50-A 12-V power supplies (Meishile) (fig. S14) and connected to two customized Arduino shield column controllers (fig. S15B) or two customized Arduino shield row controllers (fig. S15C) for column and row control, respectively. The motor driver ICs (EG Micro, EG27324) feature INA and INB pin inputs with shutdown function pins (fig. S15A). The INA and INB pins of each IC that control the actuators within the same column are interconnected and joined to two other ARM microcontrollers (Arduino Due) through insulation-displacement contact (IDC) connectors on two custom-designed Arduino shield column controller PCBs (fig. S15B). Similarly, the shutdown function pins of each IC that control the actuators within the same row are interconnected and joined to two ARM microcontrollers (Arduino Due) via screw terminals on two custom-designed Arduino shield row controller PCBs (fig. S15C). These four microcontrollers are subsequently connected to a computer wirelessly via Digi XBee modules integrated into the shields. Other peripheral components on the PCBs, including the diodes, capacitors, resistors, and light-emitting diodes, serve the purpose of circuit protection, filtering (decoupling and bypassing), power indicator lighting, and current limiting.

Foam pad, pressure-sensing mat, and dummy details

This section provides the details regarding the three items placed on top of the actuator bed (fig. S17A) as part of the actuator bed study of this work. The first item, placed on top of the actuator bed, was a 1-inch-thick (2.54-cm-thick) low-density foam pad (fig. S17B). The next item, placed on top of the foam pad, was a pressure-sensing mat from Xsensor (PX100:64.160.02) (fig. S17C). The mat consists of 160 rows and 64 columns of pressure-sensing pixels (10,240 pixels in total). Each pixel is 0.5 inches by 0.5 inches (1.27 cm by 1.27 cm) in size and can sense pressures ranging between 10 and 256 mmHg. The final item placed on top of the pressure-sensing mat was an anatomically correct dummy placed in the supine position (fig. S17D). The dummy is a 220-lb (99.79-kg) perma-gel male-body ballistic dummy purchased from the Ballistic Dummy Lab.

Mattress constituent parts and fabrication details

This section discusses the parts that constitute the AP mattress prototype of this work (Fig. 1B) and explains how the parts were fabricated. Excluding balancing springs (Fig. 3A), the 23 unique parts that constitute the mattress are shown in fig. S27A along with the

number corresponding to how many of each of those parts were made and assembled within the prototype. The six unique parts that constitute each kind of balancing spring (that is, the left-handed and right-handed balancing springs) are shown in fig. S27B along with the number corresponding to how many of each of those parts were made and assembled within each balancing spring used.

The mattress's total part count and fabrication/assembly effort will be markedly reduced for the final product when its constituent parts are injection molded and assembled like building blocks using press-fit joints as discussed previously. The current prototype's parts, shown with a yellow hue in fig. S27A and fig. S27B, were all fabricated from Vanilla White Prusament PLA filament using a Prusa i3 MK3S+ 3D printer. The metal parts, shown with a blue hue in the same figures, are all made of 1095 spring steel. Each of the four steel strips (fig. S27B), which were stacked to collectively form the compliant portion of each balancing spring (Fig. 3A), is 0.01 inches (0.0254 cm) thick and 0.75 inches (1.905 cm) wide. They were permanently bent in place using a USATCO Bendito 1824 sheet metal brake, and their bolt holes were punched using a McMaster-Carr compact portable lever-operated hole punch 3461A22. The small gray cylinders, shown in fig. S27A and fig. S27B, are nickel-plated neodymium magnets that were inserted within the posts of the mattress as shown in fig. S4A and within the mating ends of the balancing springs shown in Fig. 3A using Gorilla 5-min epoxy. The gray socket head screws and nuts, shown in fig. S27A and fig. S27B, are both made of steel. Last, the black straps (fig. S27A, Fig. 2E), which were threaded through the slits of each of the mattress's top bars (fig. S6A), are made of 0.048-inch-thick (0.12-cm-thick) and 0.5-inch-wide (1.27-cm-wide) polypropylene webbing.

Experimental setup for characterizing the mattress's performance

This section describes the setup (Fig. 5A) used to collect the pressure data from the AP mattress of this work. The setup began with a bed frame (Drive Medical Delta Ultralight 1000 Full-Electric Bed, 15033) shown in fig. S28A. A series of wooden planks that are joined together by straps made of duct tape was then placed on the bed frame (fig. S28B) followed by the AP mattress (fig. S28C). The mattress required these planks so that its underside could freely slide on their continuous low-friction surface as the bed frame's head and knee portions were raised and lowered. Without these planks, the mattress's panels and side flexures could get stuck on the uneven surface of the bed frame as it was raised and lowered. Last, the same foam pad (fig. S28D), pressure-sensing mat (fig. S28E), and dummy (fig. S28F), which were used for the actuator bed study of this work, were placed on the AP mattress in that order. A CAD image of the planks of fig. S28B is shown in fig. S29. Note that the straps interweave above and below neighboring planks in succession to achieve rolling-contact joints (*55*) between the circularly rounded sides of the planks. In this way, each plank can rotate relative to its neighbor without slipping and can thus articulate along the contour of the bed frame as it is raised and lowered. Last, note that no balancing springs were used within the mattress prototype while collecting the data of Fig. 5 because decreasing the load required to actuate the mattress was not relevant to the data collected for the plots of that figure. In addition, by not including balancing springs, an extra variable of complexity was removed from the data collection process, and all of the struts within the mattress panels were guaranteed to fully engage their corresponding hard stops.

Experimental setup for comparing the performance of the foam pad and mattress

This section describes the setup (Fig. 5B) used to collect the pressure data from a standard foam pad as a benchmark comparison with the pressure data collected from the AP mattress of this work. The setup began with the same bedframe used for the experimental setup of the mattress (fig. S28A). Large stiff wooden boards were then clamped onto the bed frame (fig. S30A) to prevent the uneven surface of the bed frame's springs from affecting the pressure data collected from the foam pad. The clamps used were fabricated from Prusa Silver PLA filament using a Prusa i3 MK3S+ 3D printer. Last, the same foam pad (fig. S30B), pressure-sensing mat (fig. S30C), and dummy (fig. S30D), which were used for the experimental setup of the mattress, were placed on the clamped wooden boards in that order.

Measuring the mattress's actuation force with balancing springs applied

This section describes the experimental setup used to measure the load required to actuate the compliant-mechanism mattress with balancing springs attached to its panels (movie S18). The measured results are also provided and discussed. The experimental setup was the same as that described in fig. S28F, with some key additional components included. The most important of those components were the balancing springs of Fig. 3A arranged within the mattress as shown in Fig. 3D. These springs were selected and placed within the mattress to optimally reduce the load required to actuate the mattress with the dummy lying on top. Care was taken to ensure that all of the supporting struts within the mattress's panels underneath the dummy engaged their hard stops but did so as gently as possible (that is, with the smallest achievable reaction load from the hard stops). A system of cords and pulleys was also constructed to the side of the mattress, as shown in Fig. 6A, to actuate it from one of its stable states to the other. Specifically, the system consists of T-slotted anodized aluminum framing, black elastic braided latex cords, ASNOMY V-groove casters that behave as pulleys, and white Delrin acetal resin tubing bars that all join within a whippletree-like mechanism that attaches to a hanging bucket in which weights could be placed to load the mattress. Eight cords on the other end of this actuation system were clipped to the foam pad underneath the pressure-sensing mat and dummy. These cords would each impart an equally distributed lateral load on the pad that collectively loaded the mattress with a force equal to the weight of the bucket and the weights placed inside.

A variety of weights were placed in the bucket to achieve different pulling loads on the mattress for 60 different actuation experiments. For each experiment, the mattress was shifted to the stable position on the side farthest away from the actuation system, as shown in Fig. 6A, by manually pulling on the dummy. The dummy was then released to identify whether the pulling load from the bucket was sufficiently high to successfully actuate the mattress to its other stable state on the side next to the actuation system. Actuation successes and failures were noted for each of the 60 experiments at each pulling load attempted and are plotted in Fig. 6B. Note from this plot that pulling loads of $\geq$19 lbf (84.5 N) have a 90 to 100% chance of successfully actuating the mattress with the 220-lb (99.79-kg) dummy lying on top. The same data are plotted as a histogram in Fig. 6C and as a logistic regression curve in Fig. 6D.

Statistical analysis

The mean, SD, and sample sizes of the data plotted in Figs. 4 and 5 are provided in their figure captions. The mean, SD, and sample sizes of the data plotted in figs. S22, S23, and S25 are provided in the Supplementary Materials in their figure captions.

Supplementary Materials

The PDF file includes:

Materials and Methods
Figs. S1 to S32
Captions for movies S1 to S18
Captions for software S1 to S3

Other Supplementary Material for this manuscript includes the following:

Movies S1 to S18
Software S1 to S3

REFERENCES AND NOTES

1. K. Agrawal, N. Chauhan, Pressure ulcers: Back to the basics. *Indian J. Plast. Surg.* **45**, 244–254 (2012).
2. M. Reddy, S. S. Gill, P. A. Rochon, Preventing pressure ulcers: A systematic review. *JAMA* **296**, 974–984 (2006).
3. E. McInnes, A. Jammali-Blasi, S. E. M. Bell-Syer, V. Leung, Support surfaces for treating pressure ulcers. *Cochrane Database Syst. Rev.* **2018**, CD009490 (2018).
4. C. Gorecki, J. M. Brown, E. A. Nelson, M. Briggs, L. Schoonhoven, C. Dealey, T. Defloor, J. Nixon, European Quality of Life Pressure Ulcer Project group, Impact of pressure ulcers on quality of life in older patients: A systematic review. *J. Am. Geriatr. Soc.* **57**, 1175–1183 (2009).
5. G. A. Duchesne, J. L. Waller, S. L. Baer, L. Young, W. B. Bollag, Pressure ulcer diagnosis is associated with increased mortality in patients with end-stage renal disease: A retrospective study. *Life* **13**, 1713 (2023).
6. S. Coleman, C. Gorecki, E. A. Nelson, S. J. Closs, T. Defloor, R. Halfens, A. Farrin, J. Brown, L. Schoonhoven, J. Nixon, Patient risk factors for pressure ulcer development: Systematic review. *Int. J. Nurs. Stud.* **50**, 974–1003 (2013).
7. M. Mansouri, G. Krishnan, D. C. McDonagh, C. M. Zallek, E. T. Hsiao-Wecksler, Review of assistive devices for the prevention of pressure ulcers: An engineering perspective. *Disabil. Rehabil. Assist. Technol.* **19**, 1511–1530 (2024).
8. Y.-K. Jan, D. M. Brienza, M. L. Boninger, G. Brenes, Comparison of skin perfusion response with alternating and constant pressures in people with spinal cord injury. *Spinal Cord* **49**, 136–141 (2011).
9. S. Pauly, P.-C. Mo, J. Elliott, A. Bleakney, S. Pappu, Y.-K. Jan, Effects of alternating pressure patterns on sacral skin blood flow responses in people with spinal cord injury. *Int. Wound J.* **21**, e14792 (2024).
10. C. H. Lyder, Pressure ulcer prevention and management. *JAMA* **289**, 223–226 (2003).
11. C. Bansal, R. Scott, D. Stewart, C. J. Cockerell, Decubitus ulcers: A review of the literature. *Int. J. Dermatol.* **44**, 805–810 (2005).
12. E. M. Landies, Micro-injection studies of capillary blood pressure in human skin. *Heart* **15**, 209–228 (1930).
13. R. S. Burk, M. J. Grap, Backrest position in prevention of pressure ulcers and ventilator-associated pneumonia: Conflicting recommendations. *Heart Lung* **41**, 536–545 (2012).
14. Y. B. Yip, A study of work stress, patient handling activities and the risk of low back pain among nurses in Hong Kong. *J. Adv. Nurs.* **36**, 794–804 (2001).
15. I. Hoogendoorn, J. Reenalda, B. F. J. M. Koopman, J. S. Rietman, The effect of pressure and shear on tissue viability of human skin in relation to the development of pressure ulcers: A systematic review. *J. Tissue Viability* **26**, 157–171 (2017).
16. E. Karvounis, S. Polymeni, M. Tsipouras, K. Koritsoglou, D. Tzovaras, "Smart beds and bedding surfaces for personalized patient care: A review" in *2021 6th South-East Europe Design Automation, Computer Engineering, Computer Networks and Social Media Conference (SEEDA-CECNSM)* (IEEE, 2021), pp. 1–8.
17. O. H. Bodine Jr., J. Wilkerson, Lateral rotation therapy mattress system and method, US Patent 5375273 (1994).
18. A. Basmajian, E. E. Blanco, H. H. Asada, "The marionette bed: Automated rolling and repositioning of bedridden patients" in *Proceedings 2002 IEEE International Conference on Robotics and Automation* (IEEE, 2002), pp. 1422–1427.
19. T. Nakamura, H. Tsukagoshi, "Soft pneumatic manipulator capable of sliding under the human body and its application to preventing bedsores" in *2018 IEEE/ASME International Conference on Advanced Intelligent Mechatronics (AIM)* (IEEE, 2018), pp. 956–961.
20. P. Pongmuksuwan, W. Harnnarongchai, Synthesis and characterization of soft polyurethane for pressure ulcer prevention. *Polym. Test* **112**, 107634 (2022).
21. Y. Yu, J. Zheng, H. Pu, C. Zhu, Q. Wu, Preparation and evaluation of an elastic cushion with waste bamboo fiber based on sitting pressure distribution of the human body. *Sustainability* **15**, 7462 (2023).
22. A. Alwasel, B. Alossimi, M. Alsadun, K. Alhussaini, Bedsores management: Efficiency simulation of a new mattress design. *Healthcare* **9**, 1701 (2021).
23. I. Moon, S.-J. Kang, G.-S. Kim, M.-S. Mun, "Control of air-cell mattress for preventing pressure ulcer based on approximate anthropometric model" in *9th International Conference on Rehabilitation Robotics, 2005. ICORR 2005* (IEEE, 2005), pp. 164–167.
24. S. Arias, E. Cardiel, L. Garay, B. Tovar, M. Pla, P. Rogeli, "A pressure distribution measurement system for supporting areas of wheelchair users" in *2013 35th Annual International Conference of the IEEE EMBS* (IEEE, 2013), pp. 4751–4754.
25. M. Bellusci, C. Ferraresi, G. G. Muscolo, "Design and control of a reclining chair with soft pneumatic cushions" in *Advances in Service and Industrial Robotics* (Springer International Publishing, 2022), pp. 239–246.
26. W. Carrigan, P. Nuthi, C. Pande, M. B. J. Wijesundara, C. S. Chung, G. G. Grindle, J. D. Brown, B. Gebrosky, R. A. Cooper, Design and operation verification of an automated pressure mapping and modulating seat cushion for pressure ulcer prevention. *Med. Eng. Phys.* **69**, 17–27 (2019).
27. G. Fiedler, G. Papaioannou, C. Mitrogiannis, G. Nianios, T. Kyprianou, "Development of a new bed system with improved decubitus prophylaxis for bed-ridden patients" in *2009 9th International Conference on Information Technology and Applications in Biomedicine* (IEEE, 2009), pp. 1–4.
28. K. H. Lee, Y. E. Kwon, H. Lee, Y. Lee, J. Seo, O. Kwon, S. W. Kang, D. Lee, Active body pressure relief system with time-of-flight optical pressure sensors for pressure ulcer prevention. *Sensors* **19**, 3862 (2019).
29. D. Mannella, M. Bellusci, F. Graziani, C. Ferraresi, G. G. Muscolo, Modelling, design and control of a new seat-cushion for pressure ulcers prevention. *Proc. Inst. Mech. Eng. H* **236**, 592–602 (2022).
30. A. Misaki, K. Imanishi, S. Takasugi, M. Wada, S. Fukagawa, M. Furue, Body pressure sensing mattress for bedsore prevention. *SEI Tech. Rev.* , 95–99 (2014).
31. P. Nair, S. Mathur, R. Bhandare, G. Narayanan, "Bed sore prevention using pneumatic controls" in *2020 IEEE International Conference on Electronics, Computing and Communication Technologies (CONECCT)* (IEEE, 2020), pp. 1–5.
32. G. Peng, L. Wang, S. Tian, Y. Fan, Modular pressure redistribution cushion with proprioceptive soft–rigid hybrid actuator. *Adv. Intell. Syst.* **6**, 2300422 (2024).
33. M. Raeisinezhad, N. Pagliocca, B. Koohbor, M. Trkov, "IntelliPad: Intelligent soft robotic pad for pressure injury prevention" in *2020 IEEE/ASME International Conference on Advanced Intelligent Mechatronics (AIM)* (IEEE, 2020), pp. 685–690.
34. J. Robinson, D. Chapman-Rienstra, J. Hong, J. Kim, H. Golecki, "Design of a custom sensing and actuating cushion for use in pressure relief in wheelchair users" in *Proceedings of the 2023 Design of Medical Devices Conference* (ASME, 2023), DMD2023-6305.
35. A. Takashima, A. Misaki, S. I. Takasugi, M. Yamamoto, Characteristic analysis of an air cell for active air mattress of prevention for pressure ulcer. *Adv. Robot.* **28**, 497–504 (2014).
36. M. Seon, Y. Lee, C. Moon, Medical robotic bed to prevent pressure sores. *Appl. Sci.* **11**, 8459 (2021).
37. R. Yousefi, S. Ostadabbas, M. Faezipour, M. Nourani, V. Ng, L. Tamil, A. Bowling, D. Behan, M. Pompeo, "A smart bed platform for monitoring & ulcer prevention" in *2011 4th International Conference on Biomedical Engineering and Informatics (BMEI)* (IEEE, 2011), vol. 3, pp. 1362–1366.
38. C. H. Yu, T. Y. Chou, C. H. Chen, P. Chen, F. C. Wang, Development of a modularized seating system to actively manage interface pressure. *Sensors* **14**, 14235–14252 (2014).
39. Z. Brush, A. Bowling, M. Tadros, M. Russell, "Design and control of a smart bed for pressure ulcer prevention" in *2013 IEEE/ASME International Conference on Advanced Intelligent Mechatronics* (IEEE, 2013), pp. 1033–1038.
40. A. Cernasov, N. Cernasov, A. Cernasov, Supporting surface with programmable supports and method to reduce pressure on selected areas of a body, US Patent 10,531,996 B2 (2020).
41. J. Elfehri, F. Boussu, V. Koncar, C. Vasseur, "Novel approach of ulcer prevention based on pressure distribution control algorithm" in *2011 IEEE International Conference on Mechatronics and Automation* (IEEE, 2011), pp. 265–270.
42. H. N. Mayrovitz, N. Sims, Effects of different cyclic pressurization and relief patterns on heel skin blood perfusion. *Adv. Skin Wound Care* **15**, 158–164 (2002).
43. D. L. Bader, The recovery characteristics of soft tissues following repeated loading. *J. Rehabil. Res. Dev.* **27**, 141–150 (1990).
44. D. A. Dzioba, K. A. Wolf, T. Wyrick, Support apparatus, system and method, US Patent US9216122B2 (2015).
45. J. S. Mervis, T. J. Phillips, Pressure ulcers: Prevention and management. *J. Am. Acad. Dermatol.* **81**, 893–902 (2019).
46. C. Y. Chai, O. Sadou, P. R. Worsley, D. L. Bader, Pressure signatures can influence tissue response for individuals supported on an alternating pressure mattress. *J. Tissue Viability* **26**, 180–188 (2017).

47. R. Fadil, B. Hoffmann, S. Lovelace, B. Farahani, S. Arzanpour, J. Loscheider, A. Aboonabi, K. Tavakolian, Design and evaluation of a dynamic air cushion for pressure ulcers prevention. *J. Tissue Viability* **31**, 491–500 (2022).
48. G. Nakagami, H. Sanada, J. Sugama, Development and evaluation of a self-regulating alternating pressure air cushion. *Disabil. Rehabil. Assist. Technol.* **10**, 165–169 (2015).
49. L. L. Howell, *Compliant Mechanisms* (John Wiley & Sons Inc., 2001).
50. S. T. Smith, *Flexures: Elements of Elastic Mechanisms* (CRC Press, ed. 1, 2000).
51. S. Soonthornkiti, P. Jearanaisilawong, Design of anti-bedsore hospital bed. *TSME J. Res. Appl. Mech. Eng.* **1**, 15–20 (2013).
52. G. Chen, S. Zhang, Fully-compliant statically-balanced mechanisms without prestressing assembly: Concepts and case studies. *Mech. Sci.* **2**, 169–174 (2011).
53. J. L. Herder, F. P. Van Den Berg, "Statically balanced compliant mechanisms (SBCM's), an example and prospects" in *Proceedings of the ASME 2000 International Design Engineering Technical Conferences & Computers and Information in Engineering Conference*, vol. 7B (ASME, 2000), pp. 853–859.
54. P. de Leva, Adjustments to Zatsiorsky-Seluyanov's segment inertia parameters. *J. Biomech.* **29**, 1223–1230 (1996).
55. S.-H. Kim, H. In, J.-R. Song, K.-J. Cho, "Force characteristics of rolling contact joint for compact structure" in *2016 6th IEEE International Conference on Biomedical Robotics and Biomechatronics (BioRob)* (IEEE, 2016), pp. 1207–1212.

Acknowledgments: Research reported in this publication was supported by the National Institute of Nursing Research of the National Institutes of Health. The content is solely the responsibility of the authors and does not necessarily represent the official views of the National Institutes of Health. Program officer K. Bough is gratefully acknowledged. B. Dicianno, from the University of Pittsburgh, is also gratefully acknowledged for the insights gleaned from his professional evaluation of our mattress prototype conducted in the Human Engineering Research Laboratories as part of the US Department of Veterans Affairs' Center for Wheelchairs and Assistive Robotics Engineering. **Funding:** This work was supported by National Institutes of Health grants 1R41NR019721-01 (J.B.H. and P.S.) and 2R44NR019721-02 (J.B.H. and P.S.). **Author contributions:** Conceptualization: J.B.H. and P.S. Fabrication: Z.Y., J.L.W., S.S., B.R., C.S., and J.C. Experimentation: Z.Y., J.L.W., and S.S. Funding acquisition: J.B.H. and P.S. Supervision: J.B.H. and P.S. Writing: J.B.H. and Z.Y. Figures: J.B.H. Movies: J.B.H. Software: Z.Y., J.B.H., and J.L.W. **Competing interests:** Some authors are inventors on the following relevant patents: issued—US 12,016,811 (J.B.H. and P.S.)—and nonprovisional applications—US 18/731,142 (J.B.H. and P.S.) and US 63/518,962 (J.B.H., P.S., Z.Y., J.L.W., and S.S.). P.S. is the founder and CEO of K Medical LLC, which intends to sell the mattress as a product once finalized. All other authors declare that they have no competing interests. **Data and materials availability:** All data and software tools are available in the main text, the Supplementary Materials, or on Zenodo at https://doi.org/10.5281/zenodo.15420682.

Submitted 21 August 2024
Accepted 21 May 2025
Published 18 June 2025
10.1126/scirobotics.ads6314

Science Robotics

Preventing pressure ulcers by increasing pressure: An unorthodox alternating-pressure mattress

Zhidi Yang, James L. Weida, Siyuan Shao, Brandon Reedel, Collin Shannon, Junlin Chen, Piyush Sheth, and Jonathan B. Hopkins

Sci. Robot. **10** (102), eads6314. DOI: 10.1126/scirobotics.ads6314

Science Robotics (ISSN 2470-9476) is published by the American Association for the Advancement of Science. 1200 New York Avenue NW, Washington, DC 20005. The title *Science Robotics* is a registered trademark of AAAS.